Periodic Focusing and Ponderomotive Stabilization of Sheet Electron Beams

J. H. Booske, A. H. Kumbasar, and M. A. Basten
Electrical and Computer Engineering Department, University of Wisconsin, Madison, Wisconsin 53706
(Received 18 August 1993)

Particle simulations compare the behavior of nonrelativistic sheet electron beams in uniform static and nonuniform time-harmonic magnetic fields. The time-harmonic fields are equivalent to periodically cusped magnetic (PCM) fields. While the sheet beam in a uniform field exhibits diocotron instability, the PCM-focused beam is stabilized by ponderomotive forces, in agreement with recent analytic predictions [J. Appl. Phys. **73**, 4140 (1993)]. Mismatched PCM-focused beams exhibit envelope oscillation and initially rapid emittance growth followed by a region of slower increase, in agreement with a recent semianalytic Fokker-Planck model.

PACS numbers: 41.85.Lc, 41.85.Ja, 52.30.Bt

Sheet or ribbon electron beams are intrinsically well suited for use where high beam currents and small beam-channel clearances are required. Applications include high-average-power free electron lasers [1], conventional low-voltage microwave tubes [2], and quasioptical gyrotrons [3]. Other applications may include gas laser excitation and high-current electron accelerators. The principal advantage of sheet beams over round cross-section beams is that by spreading the current out in the wide transverse dimension, one can propagate high currents through small beam-channel clearances without excessive space charge repulsion. The principal disadvantage of sheet beams is their susceptibility to disruption and filamentation in uniform solenoidal focusing magnetic fields. This behavior arises from $\mathbf{E}\times\mathbf{B}$ drift velocity shear and is most commonly referred to as "diocotron" instability.

Ponderomotive stabilization of instabilities is a familiar concept in plasma physics [4–6] and using ponderomotive forces to confine round cross-section electron beams is a familiar concept in accelerator physics [7,8]. As demonstrated in this Letter, periodically cusped magnetic (PCM) fields [2] provide both effective focusing and stabilization of the diocotron instability in nonrelativistic sheet electron beams.

The ponderomotive force of interest to this work is illustrated by a time-harmonic magnetic field of the form

$$\mathbf{B}(y,t)=B_0\frac{y}{L}\sin(\omega_B t)\hat{\mathbf{y}}+B_0\cos(\omega_B t)\hat{\mathbf{z}}\,. \tag{1}$$

These fields are applied to a sheet electron beam having a uniform charge density n_0, a thickness δ in the $\hat{\mathbf{y}}$ dimension, infinite width in the $\hat{\mathbf{x}}$ dimension, and uniform velocity u_0 along the $\hat{\mathbf{z}}$ dimension. The equations of motion in the transverse (x,y) plane are

$$\ddot{x}=\frac{q}{m}E_x+\omega_{cz}(t)\dot{y}-\omega_{cy}(t)u_0\,, \tag{2a}$$

$$\ddot{y}=\frac{q}{m}E_y-\omega_{cz}(t)\dot{x}\,, \tag{2b}$$

where $\omega_{cy}(t)\equiv qB_y(t)/m$, $\omega_{cz}(t)\equiv qB_z(t)/m$, and we assume that perturbations to the velocity along $\hat{\mathbf{z}}$ are negligible, i.e., $\dot{z}\approx u_0$. We proceed to solve Eq. (2) using a multiple-time-scale approach, assuming that we can separate fluctuating quantities into linear sums of fast and slow time scale responses, e.g, $x(t)=x_f(t)+x_s(t)$, $y(t)=y_f(t)+y_s(t)$, etc. The magnetic field terms (oscillating with frequency ω_B) are assumed to be varying rapidly, while the electric field terms associated with beam space charge fluctuations are considered to be slowly varying. Assuming that $u_0\gg|\dot{y}|$ and equating fast-time-scale terms yield $\dot{x}_f\approx(\omega_{c0}y_s/\omega_B L)u_0\cos(\omega_B t)$ to simplest order, where $\omega_{c0}\equiv qB_0/m$. Inserting this approximate solution back into Eqs. (2) and averaging over the fast-time motion yield

$$\ddot{x}_s\approx\frac{q}{m}E_x\,, \tag{3a}$$

$$\ddot{y}_s\approx\frac{q}{m}E_y-\overline{\dot{x}_f\omega_{cz}(t)}\approx\frac{q}{m}E_y-\left[\frac{u_0}{2}\frac{\omega_{c0}^2}{\omega_B L}\right]y_s. \tag{3b}$$

The second term on the right-hand side of Eq. (3b) represents the ponderomotive stabilizing force that survives the fast-time average. This is the force that both focuses and provides stability to the sheet beam. Proceeding as in Ref. [9], we investigate the stability of Eqs. (3) to low-frequency quasistatic perturbations of the form $\sim e^{i(kx-\omega t)}$. The quasistatic assumption combined with assuming a thin beam (i.e., $k\delta\ll 1$) leads to space charge electric terms of the form $E_x\approx-(m/2q)\omega_p^2 k\delta x_s$ and $E_y\approx(m/2q)\omega_p^2 k\delta y_s$, where $\omega_p^2\equiv n_0 q^2/m\varepsilon_0$ is the conventional beam plasma frequency. Substituting these expressions into Eqs. (3) results in normal mode solutions for the low-frequency perturbations that satisfy the relation

$$\omega\approx\pm\frac{\omega_{c0}}{2}\left[\frac{u_0}{\omega_B L}\right]^{1/2}, \tag{4a}$$

i.e., bounded, harmonic oscillation. This is in marked contrast to the result of a similar calculation [2,9] for a sheet beam in a uniform static magnetic field $\mathbf{B}=B_0\hat{\mathbf{z}}$,

$$\omega\approx\pm i\frac{\omega_p^2 k\delta}{2\omega_{c0}}\,, \tag{4b}$$

0031-9007/93/71(24)/3979(4)$06.00

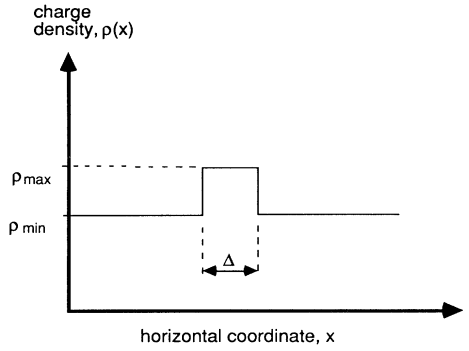

FIG. 1. Horizontal charge density distribution $\rho(x)$ with initial "square" density bunch used to initiate the diocotron instability simulation.

a purely growing perturbation.

In this Letter, we report the results of numerical particle-in-cell (PIC) simulations that demonstrate this ponderomotive stabilization of diocotron instability in sheet electron beams. Although the simulations used the time-varying fields above, their relevance to focusing in a static, spatially periodic PCM field (such as discussed in Ref. [2]) is easily established by using the transformations $\omega_B \rightarrow k_m u_0$, $u_0 t \rightarrow z$, and $L^{-1} \rightarrow k_m$, where $k_m \equiv 2\pi/l_m$ and l_m represents the spatial period of a spatially periodic magnet array.

The first simulation results illustrate the evolution of diocotron instability in a sheet electron beam immersed in a uniform solenoidal magnetic field. The initial conditions for this run included a 0.07 T uniform magnetic field (in the $\hat{\mathbf{z}}$ direction), $u_0 = 5.9 \times 10^7$ m/s (corresponding to a 10 keV beam energy), and a beam thickness of 2.0 mm. The left- and right-hand boundaries represent symmetry planes and are spaced a distance of 10.0 mm apart. The upper and lower boundaries represent conducting planes, each spaced a distance 10 mm from the midplane ($y=0$ plane) of the simulation cell. The beam charge density is uniform in the vertical ($\hat{\mathbf{y}}$) dimension. To "seed" the instability, a charge "bunch" was placed in the middle of the beam using the distribution illustrated in Fig. 1. For the ensuing diocotron instability simulation of Fig. 2, $\rho_{\max} = 3.3 \times 10^{-3}$ C/m^3, $\rho_{\max}/\rho_{\min} = 1.6$, and the bunch width was set equal to the beam thickness, i.e., $\Delta = \delta$. The meaning of these parameters is defined in Fig. 1.

The evolution of the unstable beam in configuration space is shown in Fig. 2. The vortex formation driven by the $\mathbf{E} \times \mathbf{B}$ velocity shear is clearly visible. By the end of the run (elapsed simulation time of 10 ns), filamentation is evident, as the beam has started to collect in the middle of the simulation cell and has "pulled away" from the left and right boundaries. From the simplified formula in Eq. (4b), an estimate of the diocotron e-folding time of approximately 0.5 ns is obtained—in qualitative agreement with the simulation.

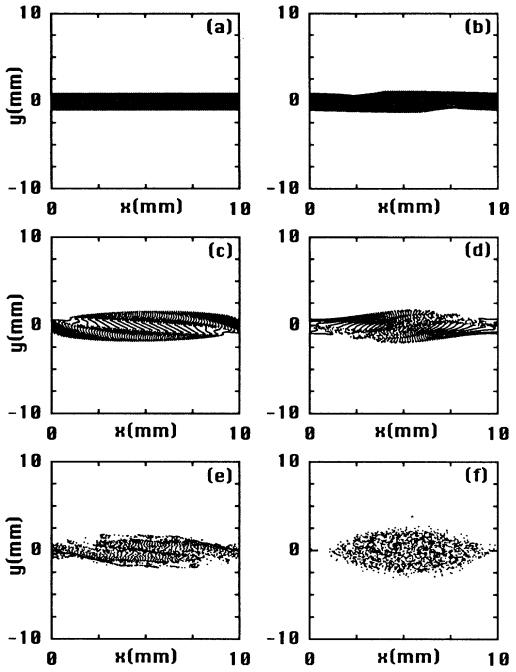

FIG. 2. Evolution of a diocotron instability for a sheet electron beam with an initial density bunch immersed in a uniform axial magnetic field of magnitude B_0. The magnetic field axis points into the page. The initial conditions were $B_0 = 0.07$ T, $\rho_{\max} = 3.3 \times 10^{-3}$ C/m^3, $\rho_{\max}/\rho_{\min} = 1.6$, $\Delta = \delta = 2.0$ mm, and $u_0 = 5.9 \times 10^7$ m/s, and the horizontal width of the simulation frame is 10.0 mm. (a) $t = 0.0$ ns, (b) $t = 0.5$ ns, (c) $t = 1.4$ ns, (d) $t = 2.8$ ns, (e) $t = 4.6$ ns, and (f) $t = 11.5$ ns.

Results obtained by repeating the above simulation with the periodic ("PCM-like") fields of Eq. (1) are presented in Fig. 3. For this example, the beam initial conditions were identical to those of Fig. 2. The peak magnetic field $B_0 = 0.07$ T, for comparison with the uniform field results of Fig. 2. The magnetic field fluctuation frequency ω_B was chosen to correspond to a PCM spatial period of $l_m \approx 5$ mm using the relations discussed above. There are three distinct features of this particular simulation case. First, the diocotron instability and filamentation observed in Fig. 2 is absent, confirming the analytic prediction. Second, the beam thickness fluctuates or "breathes" in time. This results from a ponderomotive force that initially exceeds the beam space charge forces. The effect is easily illustrated by resolving Eq. (3b)—this time for the beam envelope, $y_e(t)$, of an initially laminar, uniform (in x and y) density beam. After some algebraic manipulations, the result is [10]

$$y_e(t) = y_e(0)\left[\frac{\omega_{p0}^2}{\Omega_B^2} - \frac{\omega_{p0}^2 - \Omega_B^2}{\Omega_B^2}\cos(\Omega_B t)\right], \qquad (5)$$

an oscillatory solution, where $\Omega_B^2 \equiv u_0 \omega_{c0}^2 / 2\omega_B L$, ω_{p0} is

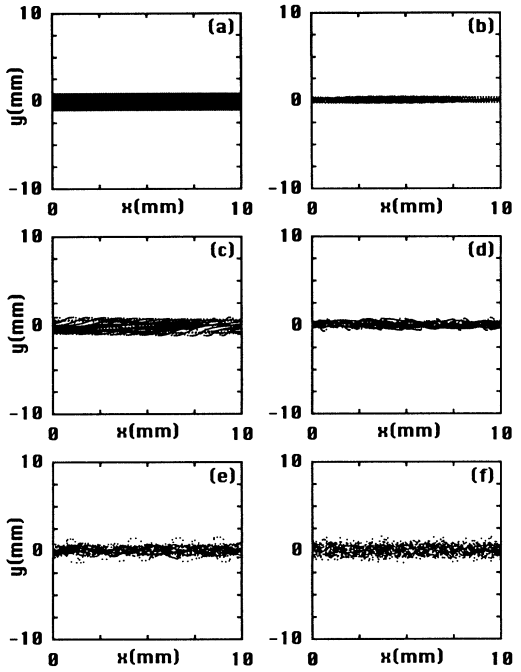

FIG. 3. Simulation demonstrating stabilization of diocotron instability by ponderomotive focusing with rapidly oscillating magnetic fields. Initial conditions for the electron beam were the same as those for Fig. 2. Parameters for the time-harmonic magnetic field included a peak amplitude $B_0=0.07$ T, a magnetic fluctuation frequency $\omega_B=1.0\times10^{11}$ s^{-1}, and a transverse gradient scale length of $L^{-1}=1.7$ mm^{-1}. (a) $t=0$ ns, (b) $t=0.5$ ns, (c) $t=0.7$ ns, (d) $t=1.2$ ns, (e) $t=1.8$ ns, and (f) $t=12.4$ ns.

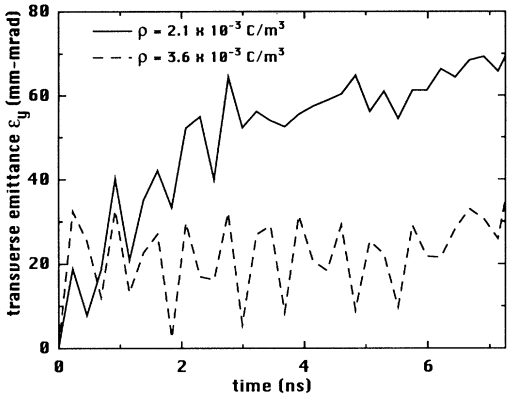

FIG. 4. Simulated evolution of emittance growth with time for ponderomotively focused sheet electron beams. The magnetic field parameters were the same as in Fig. 3. The beams were initiated as laminar, uniform density beams of thickness 2.0 mm. The solid curve displaying larger emittance growth corresponds to an initially underdense beam with $\rho(0)=2.1\times10^{-3}$ C/m^3. The lower dashed curve corresponds to an initially nearly matched beam with $\rho(0)=3.6\times10^{-3}$ C/m^3.

the initial beam plasma frequency as the beam enters the focusing channel (at $t=0$), and $y_e(0)$ is the initial beam envelope (beam half thickness at $t=0$). From Eq. (5) it is evident that if the beam enters "underdense" (i.e., $\omega_p^2<\Omega_B^2$), then the beam is compressed inwards, and the envelope oscillates with a maximum amplitude of $y_e(0)$, in agreement with Fig. 3. Finally, a significant beam "heating" or transverse emittance growth is evident from the trajectory mixing and the slight halo production of Fig. 3. This kinetic effect (not included in the simplified fluid model) has two sources: the bulk beam mismatch ($\omega_p^2<\Omega_B^2$) that gives rise to the beam envelope oscillations and the exaggerated magnitude of the initial density bunch ($\rho_{\max}/\rho_{\min}=1.6$) that was chosen to accelerate the onset of diocotron instability conditions. The second source of emittance growth is not expected to be present in a realistic, well-formed sheet beam but the first effect is certainly a realistic issue [11].

In Fig. 4, we plot the evolution of rms transverse emittance [12] $\varepsilon_y=[\langle y^2\rangle\langle\dot{y}^2\rangle-\langle y\dot{y}\rangle^2]^{1/2}$ versus time for two initially uniform, laminar sheet beams confined by the periodic magnetic fields of Eq. (1). The initial beam charge densities (for these two cases) of 2.1×10^{-3} C/m^3 and 3.6×10^{-3} C/m^3 correspond to an underdense and a nearly matched beam ($\omega_p^2\approx\Omega_B^2$), respectively. The importance of beam matching to minimize emittance growth is clearly illustrated in Fig. 4. For short PCM periods, where the period-averaged analysis presented here applies, the effective focusing force is linear [see Eq. (3b)], and the emittance growth exhibited in Fig. 4 is analogous to the well-known result for mismatched cylindrical beams [11,13]. In the case of the mismatched beam (solid trace), two regimes of emittance growth are evident, an initial, rapid growth phase lasting up to approximately 3 ns followed by a second phase of slowly increasing emittance. These results are in qualitative agreement with a semianalytic Fokker-Planck model for emittance growth of sheet beams in linear focusing channels [14]. The emittance growth for the nearly matched beam in Fig. 4 (dashed trace) is dramatically lower, as expected. Future quantitative studies of this emittance growth in ponderomotively focused sheet electron beams will provide proper estimates for phenomenological transport coefficients used in the semianalytic Fokker-Planck model.

In summary, results of numerical PIC code simulations have been presented, supporting the analytic prediction that rapidly oscillating magnetic fields can ponderomotively stabilize sheet electron beams against diocotron disruption. This technique can be experimentally realized with periodically cusped magnetic fields for nonrelativistic beams [2] and either cusped or wiggler [1] fields for relativistic sheet electron beams. In addition to stabilization, ponderomotive focusing of sheet beams must also

consider matched beam conditions to avoid unacceptably high emittance growth. Simulations comparing matched and unmatched beams illustrate this point in a dramatic fashion. In particular, the simulated emittance growth of an initially unmatched beam displays qualitative agreement with a phenomenological semianalytic Fokker-Planck model that predicts an initial phase of rapid emittance growth followed by a second phase of slower increase.

The numerical simulation results reported in this Letter were obtained using the Mission Research Corporation's MAGIC code under the AFOSR-sponsored MAGIC User's Group. The authors acknowledge considerable assistance by Dr. L. Ludeking and Dr. D. Smithe in operating the code. Appreciation is also expressed to the University of Wisconsin Engineering College's Computer-Aided-Engineering center for assistance and facilities during training sessions for use of the code. Finally, we acknowledge the University of Wisconsin College of Engineering for the purchase of the computer workstation on which these simulations were performed. This work was supported in part by the DOD Vacuum Electronics Initiative as managed by the Air Force Office of Scientific Research (Grant No. AFOSR-91-0381) and by a National Science Foundation Presidential Young Investigator Award (No. ECS-9057675).

[1] Z.-X. Zhang, V. L. Granatstein, W. W. Destler, S. W. Bidwell, J. Rodgers, S. Cheng, T. M. Antonsen, Jr., B. Levush, and D. J. Radack, "Experimental and Numerical Studies of Sheet Electron Beam Propagation through a Planar Wiggler Magnet," IEEE Trans. Plasma Sci. (to be published).
[2] J. H. Booske, B. D. McVey, and T. M. Antonsen, Jr., J. Appl. Phys. **73**, 4140 (1993).
[3] M. E. Read, A. J. Dudas, J. J. Petillo, and M. Q. Tran, in *14th International Conference on Infrared and Millimeter Waves, Wurzburg, Germany,* SPIE Conference Digest Vol. 1240 (SPIE, Bellingham, WA, 1989), pp. 79,80.
[4] J. R. Ferron, N. Hershkowitz, R. A. Breun, S. N. Golovato, and R. Goulding, Phys. Rev. Lett. **51**, 1955 (1983).
[5] G. Dimonte, B. M. Lamb, and G. J. Morales, Phys. Rev. Lett. **48**, 1352 (1982).
[6] Y. Yamamoto, S.-I. Kishimoto, H. Akimune, and T. Suita, J. Phys. Soc. Jpn. **39**, 795 (1975).
[7] V. S. Tkalich, Zh. Eksp. Teor. Fiz. **32**, 625 (1957) [Sov. Phys. JETP **5**, 518 (1957)].
[8] E. T. Scharlemann, J. Appl. Phys. **58**, 2154 (1985).
[9] O. Buneman, J. Electron. Control **3**, 507 (1957).
[10] T. M. Antonsen, Jr. (private communication).
[11] M. Reiser, J. Appl. Phys. **70**, 1919 (1991).
[12] P. M. Lapostolle, IEEE Trans. Nucl. Sci. **18**, 1101 (1971).
[13] O. A. Anderson, Part. Accel. **21**, 197 (1987).
[14] C. L. Bohn, Phys. Rev. Lett. **70**, 932 (1993).